Focused Ion Beam Writing of Optical Patterns in Amorphous Silicon Carbide

T. Tsvetkova[1], S. Takahashi[2], P. Dawson[2], A.V. Zayats[2], L. Bischoff[3], O. Angelov[4] and D. Dimova-Malinovska[4]

[1] Institute of Solid State Physics, 72 Tzarigradsko Chaussee, 1784 Sofia, Bulgaria
[2] Queen's University of Belfast, Belfast BT7 1NN, United Kingdom
[3] Forschungszentrum Dresden-Rossendorf, P.O.Box 510119, D-01314 Dresden, Germany
[4] Central Laboratory for Solar Energy, 72 Tzarigradsko Chaussee, 1784 Sofia, Bulgaria

Email contact of main author: tania_tsvetkova@yahoo.co.uk

Abstract. In the present work we investigate the use of ion beam techniques for properties modification and optimisation of wide-bandgap materials with view of their uses in sub-micron lithography and high-density data storage for archival purposes. We propose scanning near-field optical microscopy as a novel technique for characterizing the ion-implanted patterns fabricated in amorphous silicon carbide (a-SiC:H). Different patterns have been fabricated in a-SiC:H films with a focused Ga^+ -ion beam system and examined with scanning near-field optical microscopy. Although a considerable thickness change (thinning tendency) has been observed in the ion-irradiated areas, the near-field measurements confirm increases of optical absorption in these areas. The observed values of the optical contrast modulation are sufficient to justify the efficiency of the method for optical data recording using focused ion beams.

1. Introduction

Hydrogenated amorphous silicon-carbide (a-SiC:H) alloy films have been studied for many years as materials with a wide range of useful optical properties (e.g. high transparency in the visible region due to their relatively wide band-gap) [1]. Mechanical durability, chemical inertness, thermal stability, and the ease of fabrication make a-SiC:H a very promising candidate for various optoelectronic and photonic device applications in adverse environments [1, 2]. Such applications include high power microwave devices, high energy radiation detectors, UV optoelectronic, infrared nano-photonic devices as well as optical data storage [2-5]. Radio-frequency (RF) reactive magnetron sputtering (SP) is a convenient method for preparation of a-SiC:H films where, as is often the case, low density-of-states material is not required.

Ion implantation is a very attractive method for controlling the optical properties of semiconductors since the introduction of foreign elements into a host material can change the chemical composition and hence the electronic characteristics. In this way the band-gap width and related optical and electrical properties can be controlled [6]. This method is of particular interest due to the development of computer-controlled focused-ion-beam (FIB) systems, and the possibility they provide to fabricate various sophisticated ion-implanted structures [7-10].

Remarkable results have been obtained when implementing this technique to develop a new method for high-density optical data storage and sub-micron lithographic mask production using a-SiC:H films via ion-implantation of micro- and nanoscale regions [5, 10-12]. For the development of this method, use has been made of the results of conventional, broad-beam ion implantation of chemically active species, like Ge^+, Sn^+ and Ga^+, in a-SiC:H. They produce changes of the optical absorption coefficient, α, up to 1-2 orders of magnitude, depending on the ion implantation conditions. The mechanism of these changes is based on the ion beam induced structural and chemical modification of the implanted material, leading

to considerable optical bandgap decrease and hence optical absorption increase [13]. Ga^+, chosen as the implant species, is of particular interest because of its widespread use in focused ion beam systems. Studies on Ga^+ broad-beam implanted a-SiC:H films have shown various structural and chemical modification changes, leading to an effective optical bandgap decrease. The modification mechanism comprises breaking of Si-H and C-H bonds and considerable loss of H, as found by infra-red (IR) and Raman studies. These investigations also reveal increased Si-C bond breaking and formation of Si-Ga bonds, bearing in mind the lower electro-negativity of the implanted Ga atoms, as compared to the C atoms in the host material, and assuming that Ga will substitute for the C atom in the C-Si-H bond [11]. However, due to the relatively low melting point of Ga ($T_m = 29.8°C$), some proportion of the implanted Ga ions are inevitably incorporated in the form of Ga-clusters and are not directly bonded chemically to the host atoms [13]. This process will be dependent on the implantation conditions, mainly implantation temperature, and such investigations are in run.

Additionally to the changes produced in the intrinsic properties of the target material, ion implantation will also remove parts of the material, due to ablation processes [13,14]. Thus in the reported experiments on a-SiC:H thin films it is anticipated that film thinning will occur. Ion beam sputtering is relatively well understood in terms of the sputtering yield of target atoms per incident ion, depending on both the energy and ion mass of the implant beam and the mass of the target atoms. Detailed study of ablation damage has been undertaken [14], examining the effects of target temperature, dynamic changes in surface composition and the role of electronic ionization processes [15] which are expected to be only a relatively minor damage mechanism in a-SiC:H using 30 keV Ga^+ ion beams, as employed here.

As the focused-ion-beam diameter can be 10 nm or smaller, ion-implantation can be achieved in nanoscopic regions, resulting in the modification of dielectric and optical properties (transmission and reflection) of materials on this scale. Thus, high-data-density permanent archives can be recorded with optically readable information. However, in order to read data from such optical storage, a high-resolution optical technique is required. A suitable technique is scanning near-field optical microscopy (SNOM) [16] which has been successfully applied to studies of ion-beam induced modifications in silicon carbide in the infra-red [4] and visible [17] spectral ranges.

In summary, the optical density of ion implanted regions is determined by two competing contributions, mechanical thinning of the a-SiC:H film due to ion beam milling and modification of the film properties (i.e. increased optical absorption) due to ions implanted in the film. Thus, studies of both topographic and optical properties of thin films are important to optimize the ion implantation processing for optical data storage applications. In this investigation the simultaneous mapping of topography and optical contrast is achieved using a SNOM instrument.

In order to characterize the optical properties of micro- and nano-scale structures, a "super-resolution" technique is required. In addition, ion irradiation may cause ablation of the a-SiC:H film, leading to changes of the topographic features of the surface. From this point of view, scanning near-field optical microscopy (SNOM) [16], with the shear force technique that provides topography data, is a promising method that can obtain both optical and topographic images of the sample simultaneously. In this work, a focused Ga^+-ion beam system has been used to create micron-scale optical patterns in a-SiC:H films. The patterning process has been studied applying SNOM techniques to investigate topographic as well as optical variations of the modified surface.

2. Experiment

Thin films of a-Si$_{1-x}$C$_x$:H (x = 0.15) were deposited onto glass substrates with 13.56 MHz radio-frequency (RF) reactive magnetron sputtering. A target composed of a mono-crystalline (100) silicon wafer with chips of pure graphite placed on it, was sputtered in an Ar-20%H$_2$ gas mixture. Typical deposition conditions were an RF power of 150 W (power density 1.91 W cm^{-2}), a total gas pressure of 1 Pa, a substrate temperature of 275°C, and a graphite-to-silicon target ratio of 0.025. The film thickness was measured to be approximately 200 nm.

Focused Ga$^+$-irradiation in these samples was performed with a FIB system (CANION 31Mplus column, Orsay Physics) to implant sub-micron optical patterns in the a-SiC:H films. The chess-board-like (CBL) and series of lines (SL) patterns were thus created with different ion doses in the range $8.0 \times 10^{14} - 3.2 \times 10^{16}$ ions cm^{-2}. These conditions allow one to achieve line-widths of implanted areas as small as 200 nm [11]. The choice of the Ga$^+$ ion dose range has been prompted by earlier results [11], where the optimized range of ion doses for Ga$^+$ and other elements has been established to be 1×10^{15} to 1×10^{17} ions cm^{-2} to yield a good optical contrast. Thus, in the samples studied, Ga$^+$ ion doses are chosen within this range.

The patterns obtained were characterized by SNOM technique. Simultaneous topographic and optical data was obtained with SNOM measurements using a custom-built microscope in transmission mode. The details of the SNOM measurements are described in our previous work [12,17] and the references therein. Briefly, an unpolarised beam from a He-Ne laser (633 nm) illuminates the substrate-side of the sample. The laser is not focused in order to keep the laser intensity on the scanned area as uniform as possible. Light passing through the patterned area is collected by a sharp, uncoated optical fibre probe from one point to the next, in order to form optical near-field images. The gap between the probe end and the sample is kept constant with a non-optical shear-force technique that employs a quartz tuning fork; feedback from the shear-force regulation scheme yields topographic information. Topography and local optical mapping are thus achieved simultaneously.

3. Results

Fig. 1 shows an optical micrograph of an a-SiC:H thin film with a variety of patterns created with FIB. They consist of chess board like (CBL) and series of lines (SL) patterns with different doses. Due to the ion implantation the optical density of the irradiated areas is increased so that they are seen as dark regions.
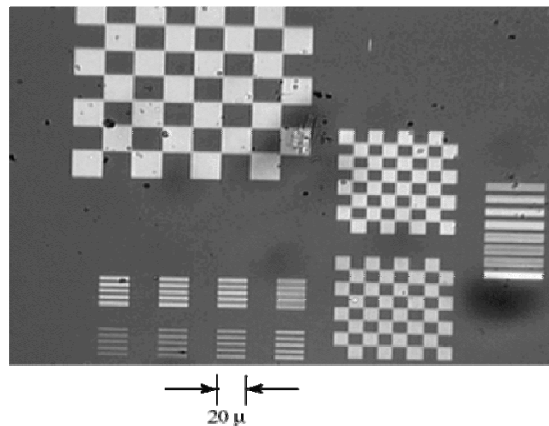

FIG. 1: *Optical contrast pattern, written with the IMSA-Orsay Physics FIB, using a 15 pA Ga beam into a-SiC:H film. The size of the big chess field is 20 x 20 μm^2.*
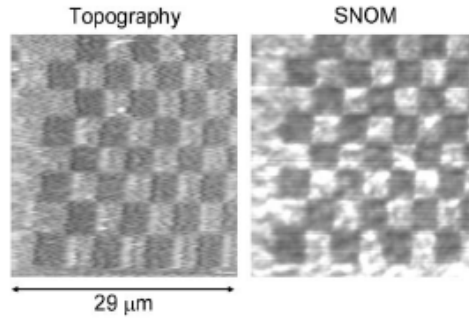
FIG. 2. Topographic image and corresponding SNOM optical image of a chess board like pattern created on an a-SiC:H thin film with the IMSA-OrsayPhysics FIB using a 15pA Ga beam

As already mentioned in the introduction, SNOM can provide simultaneously the optical images together with the corresponding topographic images of the patterns (Fig.2). Fig. 3 shows simultaneously obtained topographic and near-field optical images of a series of 8 stripes, made by FIB-implantation in an a-SiC:H film with different ion doses, *D,* which are specified in Table I. All structures were implanted at an ion energy E = 30 keV. For this energy the values for the mean projected range R_p and the straggle ΔR_p were calculated using the SRIM code [18], to be R_p = 18.6 nm and ΔR_p = 6.2 nm, respectively. Estimations of the resulting mean concentration per unit volume, N_V (ions cm^{-3}) and the atomic concentration, N_A (at%) are also given in Table I below [19], excluding effects of preferential sputtering. Whilst such predictions of the average Ga concentration are reliable, they do not include information on how the Ga is incorporated within the host and so ignore probable Ga precipitation effects.
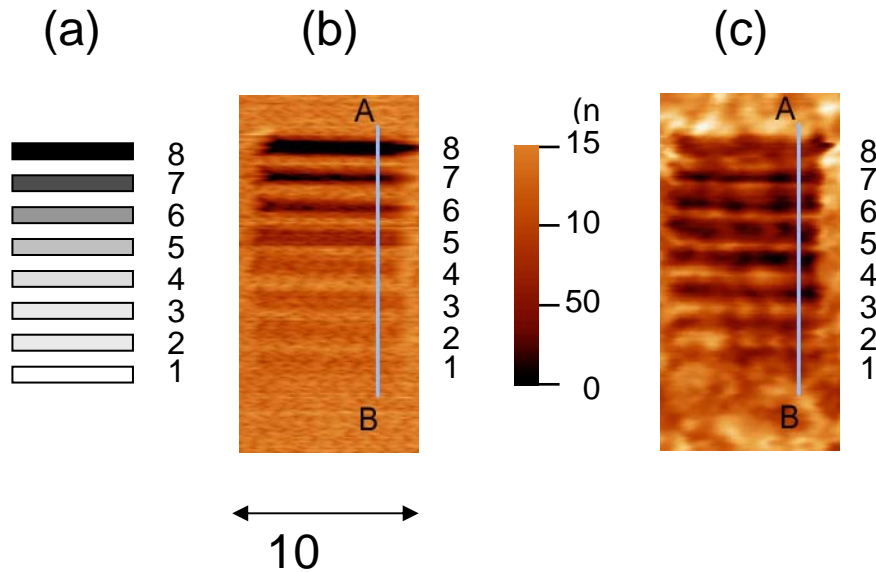

FIG. 3.   (a) Schematic illustration of the pattern fabricated on the surface of a-SiC:H with FIB Ga$^+$ ion implantation; (b) topography obtained using shear-force imaging in the SNOM, and (c) simultaneously measured near-field optical image.

The ion dose used in Fig. 3 is highest for the top stripe (#8), decreasing to the bottom one (#1). Ion irradiated areas are topographically thinner, while the local transmission measured with SNOM above the corresponding region is weaker, due to the increase of optical density associated with the ion implantation. It should be noted that for the stripes with the low implantation dose, the topography changes are not very significant and difficult to distinguish on the background of spurious topography variations related to the intrinsic film roughness.

Typical cross-sections (along the line AB) in the topographic and optical images are presented in Fig. 4. The errors in the topographic and optical data, based on calculation of the standard deviation in various regions of the surface, are approximately ±2.5 nm and ±(0.02-0.03) arbitrary units, respectively; clearly the changes (relative to the local background) associated with stripes 1 and 2 in particular are subject to quite a large percentage error. The implantation dose for each line decreases from left to right in the cross-sectional plot. While the topographic contrast decreases from the left (higher doses) to the right (smaller doses), the corresponding near-field transmission exhibits a more complex behavior. Whilst the optical transmission is decreased in the implanted regions, relative to the signals in the unimplanted areas, the transmission maxima between the implanted zones do not return to the same high level as in the unimplanted regions. Secondly, the minima in transmission do not fall monotonically with dose. In fact, the values for the minima are relatively constant for doses of about 3.0×10^{15} to 1.6×10^{16} ions cm^{-2}.

TABLE I: Implantation doses, D, volume concentration, N_V and atomic concentration, N_A, for the pattern of lines (assuming thickness of implanted layer $d = 2\,\Delta R_p = 12.40$ nm [18])

| Line No	D [ions cm^{-2}]	N_V [ions cm^{-3}]	N_A [at %]
1	8.0×10^{14}	6.45×10^{20}	0.11
2	1.6×10^{15}	1.29×10^{21}	0.21
3	3.2×10^{15}	2.58×10^{21}	0.43
4	5.0×10^{15}	4.03×10^{21}	0.67
5	8.0×10^{15}	6.45×10^{21}	1.07
6	1.3×10^{16}	1.05×10^{22}	1.74
7	1.6×10^{16}	1.29×10^{22}	2.14
8	3.2×10^{16}	2.58×10^{22}	4.28
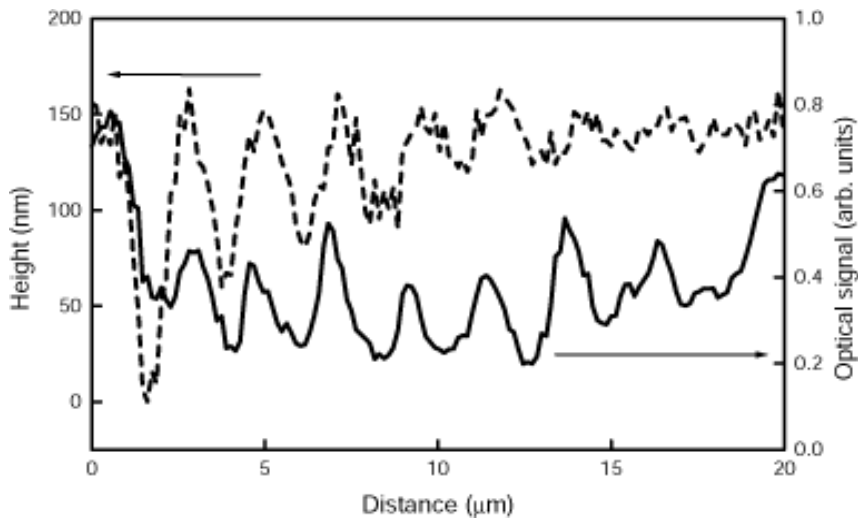
FIG. 4.   *Cross sections, representing the average of 4 line scans, of the topographic and optical images taken along the line-cut AB in figure 1, i.e. the features indicated as 8 through 1 in figure 1 run from left to right in the cross sections shown here*

In order to investigate these changes quantitatively, the topographic change, (i.e. change in thickness relative to the unperturbed sample thickness) and optical contrast, C_{opt}, are plotted as a function of the dose, D, in Fig. 5 where the optical contrast is defined as:

$$C_{opt} = \left(\frac{I_u - I_i}{I_u} \right) \qquad (1)$$

Here I denotes the transmitted intensity with the subscripts u and i depicting the unimplanted and implanted regions respectively. The quantity I_u is evaluated from an average of the peaks on each side of a minimum, except for the cases of the first and last minima (corresponding to the heaviest and lightest doses) where only the 'inner' peak in the ion implanted section of the sample is used; the recovery to higher transmission levels in unperturbed regions of the sample otherwise distorts the contrast measures for the first and last minima. It is notable from Fig.5 that the ion implanted thinner regions of the sample are less optically transmissive. While the magnitude of the topographic change increases almost linearly with ion dose, the optical contrast reaches a maximum of 0.58 at $D = 3.0 \times 10^{15}$ ions cm^{-2} and then decreases with higher doses (with an anomalous point at $D = 5.0 \times 10^{15}$ ions cm^{-2}).
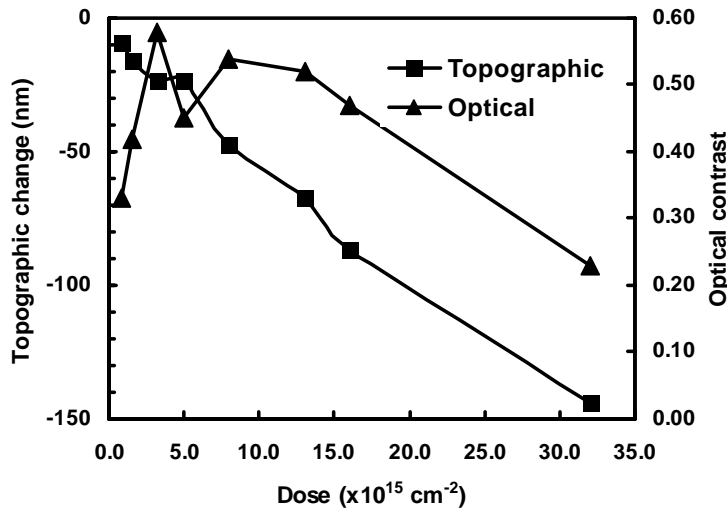
FIG. 5. *Dependence of the topographic variation and optical contrast of ion irradiated a-SiC:H on the Ga$^+$ ion dose plotted from Figs.3 and 4. The solid lines are guides for the eye.*

4. Discussion

When a film surface is irradiated with an ion beam, there are two possible processes: implantation of the ions into the film [6,13] and ablation of the film [6,13,14]. The increase of the optical density is caused by the former process, while topographic thinning results from the latter. The ablation may also limit the maximum absorption that can develop since sputtering of Ga will define an upper limit to the amount of ions that is retained. The result of Fig. 5 implies that at lower doses the ion implantation prevails over the ablation effect. The implantation reaches its saturation at a dose $D = 3.0 \times 10^{15}$ ions cm^{-2}. For doses larger than this value, the ablation effect starts to outdo the implantation effect. Given that the initial thickness of the a-SiC:H layer is ~200 nm, topographical thinning of 150 nm (for the highest dose) implies a residual a-SiC:H layer of only ~50 nm thickness. Nevertheless, film thinning alone, even by 150 nm for the highest dose, cannot account for the lack of increase in the optical contrast for $D > 10^{15}$ ions cm^{-2} as the residual thickness of 50 nm is still considerably greater than the estimated mean projected range of ~20 nm for the 30 keV ion beam energy.

The key feature that must be noted for a practical device is not the level of absorption achieved by the implant, but the contrast that develops relative to the immediately adjacent regions. Local optical measurements are of particular importance in this respect as they provide a way to study how sharp the optical contrast change is between the implant zones and nominally unaffected regions between them. Inspection of Fig. 4 shows (in arbitrary units) that at the zero-dose end of the scale a high transmission factor of > 0.6 units is obtained, but that this drops to ~ 0.4 units over most of the range and rises again in the zone beyond the highest implant. Crucially, the transmission values of ~0.4 are those which define the optical contrast against the transmission values in the implanted regions of ~ 0.2 units. This lack of recovery of the transmission to ambient levels associated with unperturbed regions of the sample is indicative of non-local damage and this is not unexpected for several reasons:

- There is diffusion and loss of Ga from the implanted region, leading to modification of the interzone 'reference' regions.

- Surface heating will have a direct influence on the movement and loss of hydrogen from the a-SiC:H as well as influencing the diffusion and nanoparticle formation of the gallium. These features will affect the optical properties and will spread beyond the immediate implant region, even for a material with high thermal conductivity like a-SiC:H. Note that the operating conditions of the FIB imply a power density on the surface of the order of kW cm^{-2}.

- Internal stress in the a-SiC:H due to the above Ga- and H-related compositional factors will also extend beyond the implant regions, influencing the optical properties. This applies particularly to stress terms arising from volume changes associated with gallium precipitates. From earlier glass studies, factors which controlled the reflectance were linked to the fact that Ga has a very low melting point ($T_m = 29.8°$C) and possesses the unusual feature of volume contraction on melting. Such factors favor Ga incorporation as dispersed clusters, or small nanoparticles [13,20] with the concomitant of large associated internal stress in the host material.

Finally, there are two further points of note. First, in addition to the contrast limitation in the striped region due to the intrinsic material factors discussed above, there will be some influence of the instrumental resolution associated with the SNOM, especially with the use of uncoated fibres. Secondly, as a point of background, it is notable that the change in optical absorption is somewhat less than the order of magnitude change obtained in conventional far-field optical measurements in the ultraviolet from samples implanted with an unfocused, broad ion beam. The large ultraviolet contrast arises from amorphisation changes in the host material, but these are relatively unimportant here; instead the transmission changes are more strongly influenced by the presence of Ga itself and the formation of nanoscale precipitates [20]. Moreover, surface temperature-enhanced sputtering (including that of the Ga implant) from the regions exposed to the ion beam will act to limit the transmission change achievable.

In summary, the optical contrast achieved, even at relatively low doses, is of sufficient magnitude to be useful in high-density optical data storage and sub-micron lithographic mask production. This result is of considerable importance when estimating the cost effectiveness of the method, lower doses implying less costly implantation time. The resolution achievable by this method will be defined by the diameter of the Ga$^+$ focused ion beam and the region of collateral modification/damage, similar to proximity effects in electron beam patterning, but, nonetheless, should offer a significant improvement over the resolution determined by the diffraction limit of light in optical lithography.

5. Conclusion

In conclusion, SNOM has been used to study the topographic and optical contrast changes in ion irradiated a-SiC:H films. The results show that at lower doses, the ion implantation leads to increased absorption and, therefore, higher optical contrast. At higher doses, the optical absorption saturates and further ion irradiation causes a decrease in optical contrast due to the ablation of the thin film. The present study thus shows the existence of optimal implantation conditions of a-SiC:H films to achieve large optical contrast with less topographic change. Low ion doses are sufficient and preferable for achieving strong optical absorption change, which is needed for application in optical data storage for creating permanent optical archives.

Acknowledgments

References

[1]   POWELL, J.A., MATUS, L., Amorphous and Crystalline Silicon Carbide, (HARRIS, G.L. and YANG, C.Y.W., Eds.), Springer, Berlin, 1989.
[2]   KANICKI, J., (Ed), Amorphous and Microcrystalline Semiconductor Devices, Artech House, Boston, 1991.
[3]   KILDEMO, M., Thin Solid Films, **455-456** (2004) 187.
[4]   OCELIC, N., HILLENBRAND, R., Nature Materials, **3** (2004) 606.
[5]   KALBITZER, S., Curr. Opin. Solid State Mater. Sci., **6** (2002) 271.
[6]   HIRVONEN, J.K., Ion implantation and ion beam processing of materials, North Holland, Amsterdam, 1984.
[7]   BÖHRINGER, K., JOUSTEN, K., KALBITZER, S., Nucl. Instrum. Methods B, **30** (1988) 289.
[8]   RUTTENSPERGER, R., KRÖTZ, G., MÜLLER, G., DERST, G., KALBITZER, S., J. Non-Cryst. Solids, **137-138** (1991) 635.
[9]   BISCHOFF, L., Ultramicroscopy, **103** (2005) 59.
[10] MÜLLER, G., Nucl. Instrum. Methods B, **80-81** (1993) 957.
[11] TSVETKOVA, T., TZENOV, N., TZOLOV, M., DIMOVA-MALINOVSKA, D., ADRIAENSSENS, G.J., PATTYN, H., Vacuum, **63** (2001) 749; BISCHOFF, L., TEICHERT, J., KITOVA, S., TSVETKOVA, T., Vacuum, **69** (2003) 73.
[12] TSVETKOVA, T., TAKAHASHI, S., ZAYATS, A.V., DAWSON, P., TURNER, R., BISCHOFF, L., ANGELOV, O., DIMOVA-MALINOVSKA, D., Vacuum, **79** (2005) 100.
[13] TOWNSEND, P.D., CHANDLER, P.J., ZHANG, L., Optical Effects of Ion Implantation, Cambridge University Press, Cambridge, 1994 (revised 2006).
[14] KNYSTAUTAS, E. (Ed.), Engineering thin films and nanostructures with ion beams, Taylor and Francis, Boca Raton, 2005.
[15] TSVETKOVA, T., SELLIN, P., CARIUS, R.., ANGELOV, O., DIMOVA-MALINOVSKA, D., J. Optoelectronics and Advanced Materials, **9** (2007) 375.
[16] RICHARDS, D., ZAYATS, A.V. (Eds), Nano-optics and near-field microscopy, Phil. Trans. R. Soc. London, **362** (2004) 699–812.
[17] TSVETKOVA, T., TAKAHASHI, S., ZAYATS, A.V., DAWSON, P., TURNER, R., BISCHOFF, L., ANGELOV, O., DIMOVA-MALINOVSKA, D., Vacuum, **79** (2005) 94.
[18] MAYER, J.W., ERIKSON, L., DAVIES, J.A., Ion implantation in semiconductors, Academic Press, New York, 1970.
[19] KALBITZER, S., Nucl. Instrum. Methods B, **218** (2004) 343.
[20] HOLE, D.E., TOWNSEND, P.D., BARTON, J.D., NISTOR, L.C., VAN LANDUYT, J., J Non-Cryst. Solids, **180** (1995) 266.